Progress In Electromagnetics Research M, Vol. 105, 151–160, 2021

Influence of Materials, Windows and Shielding Layers on Low-Frequency Electromagnetic Environment of Subway Vehicle and Human Exposure Research

Zhi Yuan Wang[1, *] and Wei Nan Liu[2]

Abstract—The numerous high-power devices and cables gathered around the subway vehicle will aggravate the deterioration of the electromagnetic environment, which may cause the train to fail to operate normally or threaten the health of passengers with a pacemaker or defibrillator. In order to study the distribution characteristics of low-frequency magnetic field of the subway in complex electromagnetic environment and the influence of various factors on human electromagnetic exposure, the magnetic flux density nephograms of the subway train with different vehicle body materials, with or without windows and with the shielding layer are calculated and analyzed. Specific energy absorption rate (SAR) values have been calculated in a standing voxel model from exposure to electromagnetic fields at 2.4 GHz, frequencies commonly used by Wi-Fi devices. The numerical results show that the average value of magnetic flux density in the stainless-steel carriage is less than that in the aluminum alloy carriage and the carbon fiber reinforce plastic (CFRP) carriage. Compared with the vehicle with windows, the average value of magnetic flux density in the vehicle without windows is less. The added shielding layer decreases the average value of magnetic flux density from 10.5 μT to 3 μT. The maximum value of magnetic flux density in the carriage under different factors is about 10 μT, which is far less than the magnetic flux density reference limit of 0.1 mT of the International Commission of Non-Ionizing Radiation Protection (ICNIRP) standard. When the Wi-Fi device is closest to the human body, the highest Specific Absorption Ratio (SAR) value of human tissue is 0.00749 W/kg, which is far less than the electromagnetic exposure limit of 1.6 W/kg of IEEE standard.

1. INTRODUCTION

With the rapid growth of economy, urban subway, light rail, and other rail transit have been developed fast. At the same time, the safety of the train and the health of passengers attract much attention. As a complex giant system, subway train has numerous high-power devices and cables. These interference sources will transmit electromagnetic wave, which will aggravate the deterioration of the electromagnetic environment inside and outside the vehicle. If the electromagnetic field value in the subway train exceeds the value of the relevant standards, there may be interference with the body wearable or implanted devices such as pacemaker and defibrillator [1, 2]. Therefore, it is of great significance to predict the low-frequency electromagnetic field distribution of the subway train and study human electromagnetic exposure in the subway vehicle.

At present, the main research contents of rail transit electromagnetic environment are mostly focused on the calculations and analysis of a certain subsystem [3–5], and the analysis of the overall electromagnetic environment of the vehicle body is relatively deficient. Paper [6] discusses the electromagnetic situation in the internal space of the engine nacelle during the emission of

Received 4 August 2021, Accepted 1 November 2021, Scheduled 2 November 2021
* Corresponding author: Zhi Yuan Wang (wangzhiyuan@stu.xupt.edu.cn).
[1] Xi'an University of Posts and Telecommunications, China. [2] Oregon State University, USA.

electromagnetic interference from the generator power lines. In [7], the low-frequency electromagnetic field distribution of high-power cable in cabinet is predicted. At frequencies higher than 100 kHz, the primary cause of damage to the human tissues from electromagnetic exposure is due to heating effects and nonelectro-stimulation [8]. In bioelectromagnetic field, the health and safety issues related to RF electromagnetic radiation have attracted much attention. The heating effect on the tissues is usually quantified by Specific Absorption Rate (SAR) [9]. And the SAR value should not exceed the limit specified in the standard. The International Commission on Non-Ionizing Radiation Protection (ICNIRP) [10] and IEEE [11] have set the safety standards for human protection and electromagnetic fields protection. Some scholars have studied the interaction of electromagnetic fields and human exposure [12–14] and methods for SAR measurement [15]. Hence, it is important to study the exposure levels and avoid tissue damage due to electromagnetic radiation.

The paper establishes the detailed models of the carriage and human body, and predicts the low-frequency magnetic field distribution of the vehicle in a complex electromagnetic environment by FEKO software. Considering the fact that ordinary methods consume a lot of computing resources and time, Multi-Layer Fast Multipole Method (MLFMM) is selected to calculate the low-frequency magnetic field in the vehicle. The distribution of low-frequency magnetic field in the vehicle under different factors is calculated, and the results are compared with the standards defined by ICNIRP and IEEE. Then SAR values at different distances between the device and the human model have been calculated in a standing voxel model from exposure to electromagnetic fields at 2.4 GHz, frequencies commonly used by Wi-Fi devices. The calculated results are compared with the exposure limit specified by ICNIRP to analyze the safety of the electromagnetic exposure to human health.

2. ESTABLISHMENT OF MODELS

2.1. Establishment of the Vehicle Model

The vehicle body structure is composed of a roof, a left-side wall, a right-side wall, inside and outside end walls, and the vehicle bottom. Under the vehicle bottom, there are models of traction motors, an auxiliary invertor, a traction invertor, and a brake resistor. Besides the bottom parts, the vehicle body model includes pantograph, high-tension cable, carriage, and windows. The length, width, and height of the vehicle model are respectively 22.4 meters, 3.3 meters, and 2.8 meters. In order to simplify the model of vehicle body, the metal material with air sandwich is simplified to a single metal plate of 5 centimeters thickness. The vehicle model and important devices are shown in Figure 1.

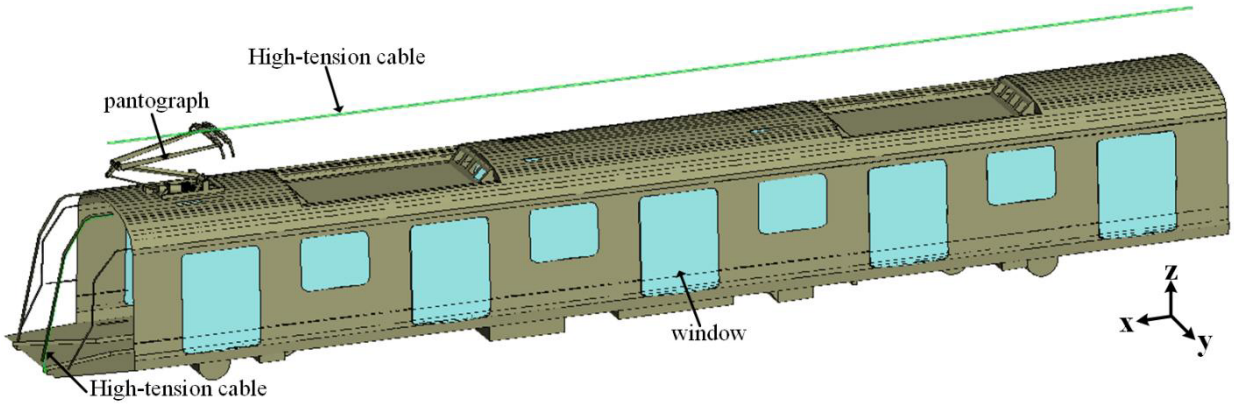

Figure 1. The model of the vehicle body.

2.2. Setting of the Interference Source

In the subway, the main interference sources are high-tension cables and a series of high-power equipment such as traction inverter and traction motor suspended under the carriage. The simulation is carried

out under the condition that the cable has no shielding at all. According to the path of current flowing from the pantograph to the ground, the paper sets the current value as 300 A. In addition, a series of high-power equipment such as traction inverter and traction motor is placed under the carriage, which are also the main interference sources of subway trains. In order to simplify the simulation, we use two symmetrical magnetic point sources replacing traction inverter and traction motor as the interference source (near-field source) of the subway. The center coordinates are respectively (2.5, 0, 0.5) and (−2.5, 0, 0.5). The value of magnetic point source is 10 Am^2, and its magnetic field is along the positive Z direction. The location of magnetic point source is shown in Figure 2.

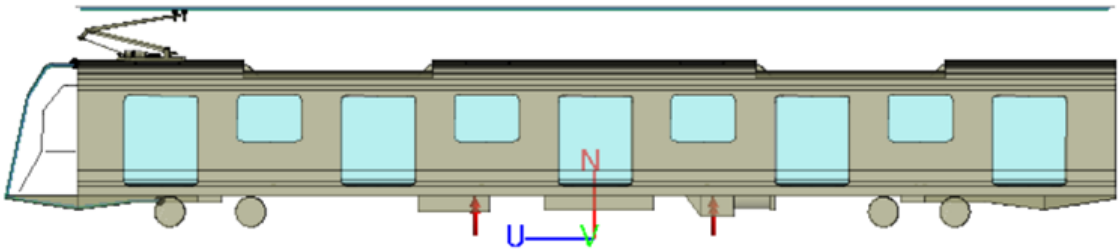

Figure 2. The location of magnetic point source.

To analyze the magnetic field distribution inside the vehicle, the sections are divided at the heights of 0.9 m and 1.5 m from the vehicle floor according to the measurement method of low-frequency magnetic field in the subway vehicle [16]. The heights of 0.9 m and 1.5 m are about the heights of the heart from the floor when an adult is sitting and when standing, respectively.

2.3. Establishment of the Human Body Model

In the field of bio-electromagnetics, human models with high resolution and accurate electrical parameters are often used for numerical calculations. When human body is exposed to electromagnetic field, it is impossible to obtain the distribution of physical quantities such as magnetic induction intensity and induction electric field intensity in various tissues by external equipment. For this kind of problem, the general method is based on the principle of electromagnetic dosimetry, using the numerical calculations method to quantitatively analyze the distribution of electromagnetic field in human tissues. In the paper, an adult female model of Computer Simulation Technology (CST) was used to study human electromagnetic exposure. The human model and human anatomy are shown in Figure 3. In order to observe the influence of different electromagnetic environments on human electromagnetic exposure, it is necessary to set corresponding biological dielectric parameters for different tissues of the human body model. The relative permittivity, conductivity, and mass density of main human tissues at 2.4 GHz are shown in Table 1.

Table 1. Relative permittivity, conductivity and mass density of human main tissues at 2.4 GHz.

Biological tissues	Relative permittivity	Conductivity (S/m)	Mass density (kg/m^3)
Heart	2.2159	54.918	1059
Liver	1.6534	43.118	1050
Lung	1.6486	48.454	563
Brain	1.48145	42.61	1035.5
Trunk	0.697	37.67	1454.5

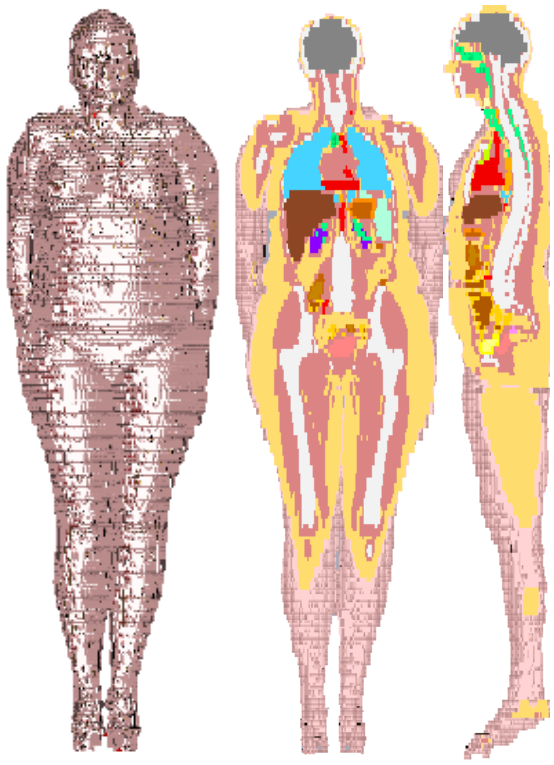

Figure 3. The human model and human anatomy.

3. INFLUENCE OF DIFFERENT FACTORS ON LOW-FREQUENCY MAGNETIC FIELD

3.1. Influence of the Vehicle Body Materials on Low-Frequency Magnetic Field

Subway vehicle body materials are changing from stainless steel to aluminum alloy, and then to composite material. It is very important to study the influence of vehicle body materials on the low-frequency magnetic field environment of subway. In this paper, aluminum alloy, stainless steel, and carbon fiber reinforce plastic (CFRP) materials are assigned to the vehicle body materials, and the distribution of magnetic flux density in the vehicle is observed with other settings unchanged. The conductivity and relative permeability of the three materials [17] are shown in Table 2.

Table 2. Electromagnetic parameters of the three materials.

Materials	Conductivity (S/m)	Relative permeability
Stainless steel	1.441e + 06	1500
Aluminum alloy	2.857e + 07	1
CFRP	4.290e + 05	539

The distributions of magnetic flux densities at 0.9 m above the floor in the subway vehicle with three vehicle body materials are shown in Figure 4. The average values of magnetic flux densities, in the stainless-steel carriage, the aluminum alloy carriage, and the CFRP carriage, are about 5.4 μT, 6.3 μT, and 5.8 μT, respectively. The overall value of magnetic flux density of the stainless-steel carriage is also lower than that of the aluminum alloy carriage and CFRP carriage. However, the maximum value of magnetic flux density of the three materials is 10 μT, which is far less than the magnetic flux density reference limit of 0.1 mT at 50 Hz defined by of the ICNIRP standard.

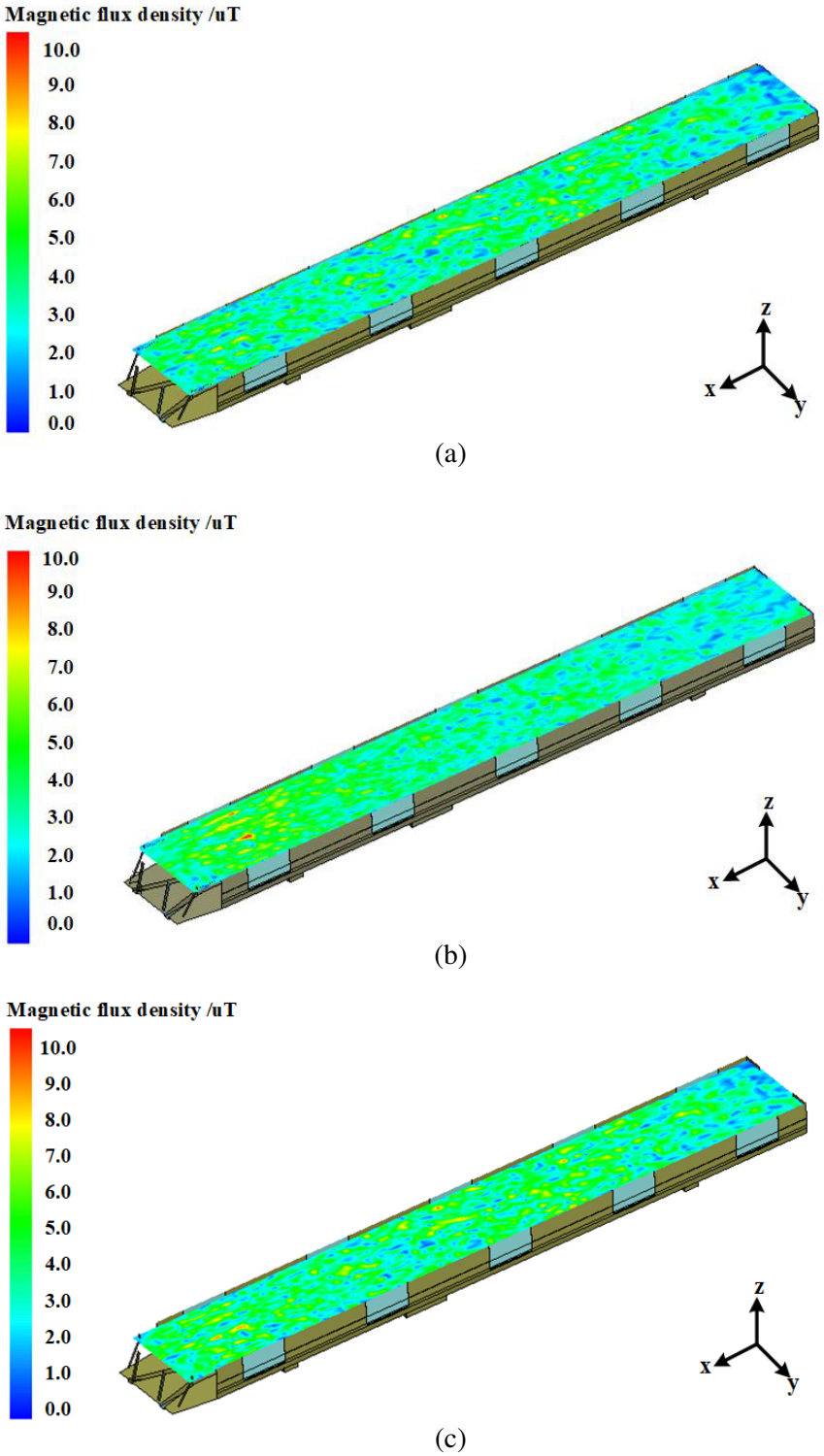

Figure 4. The nephogram of magnetic flux density in the vehicle with different materials. (a) Stainless steel. (b) Aluminum alloy. (c) CFRP.

3.2. Influence of the Windows on Low-Frequency Magnetic Field

The low-frequency magnetic fields are not easily distorted by metals normally used for the vehicle body and other objects inside the vehicle. This may be different when stainless steel is used. In the paper, the

glass material of the subway vehicle is changed to stainless steel material with other settings unchanged. It is similar to subway vehicle without windows. The distributions of magnetic flux densities at 0.9 m above the floor in the subway vehicle with and without windows are shown in Figure 5. The average value of magnetic flux density in the carriage with windows is about 5.4 μT. And the average value of magnetic flux density in the carriage without windows is about 4.9 μT. However, the maximum value of magnetic flux density of the vehicles with or without windows is far less than the magnetic flux density reference limit of 0.1 mT at 50 Hz defined by of the ICNIRP standard.

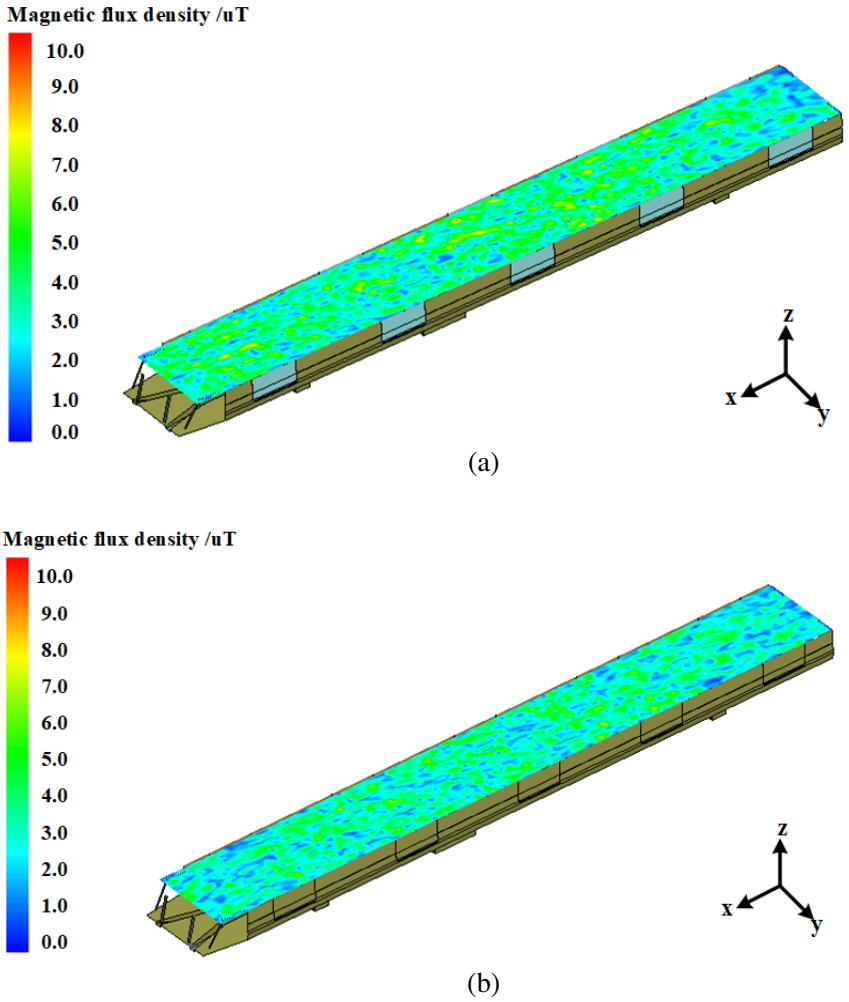

Figure 5. The nephogram of magnetic flux density in the vehicle with or without windows, (a) with windows, (b) without windows.

3.3. Influence of the Shielding Layer on Low-Frequency Magnetic Field

Electromagnetic shielding is an effective method to solve the electromagnetic compatibility problem and to suppress the radiation interference. In the paper, the roof material of the model is modified to the stainless steel, and the stainless-steel shielding layer is set at the rear of the cockpit. Through the simulation calculations, the distribution of magnetic flux density at 0.9 m above the floor in the subway vehicle is shown in Figure 6. After adding the shielding layer, the electromagnetic environment in the vehicle is obviously improved, and the average value of magnetic flux density decreases from about 10.5 μT to 3 μT.

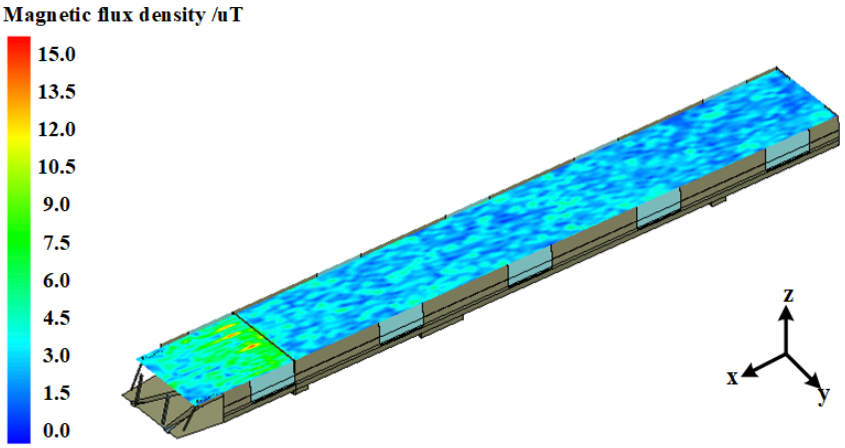

Figure 6. The nephogram of magnetic flux density in the vehicle with the shielding layer.

4. INFLUENCE OF WI-FI DEVICE ON HUMAN ELECTROMAGNETIC EXPOSURE

With the development and research of Wi-Fi equipment in subway, the research on the electromagnetic safety impact on human body in the process of using equipment is gradually carried out. Whether the electromagnetic field generated by the mutual transformation of magnetic field and electric field will affect biosafety is very important. Passengers can use convenient Wi-Fi devices to achieve wireless accessing internet in subway trains without Wi-Fi hot spots. The 2.4 GHz band is adopted for Wi-Fi

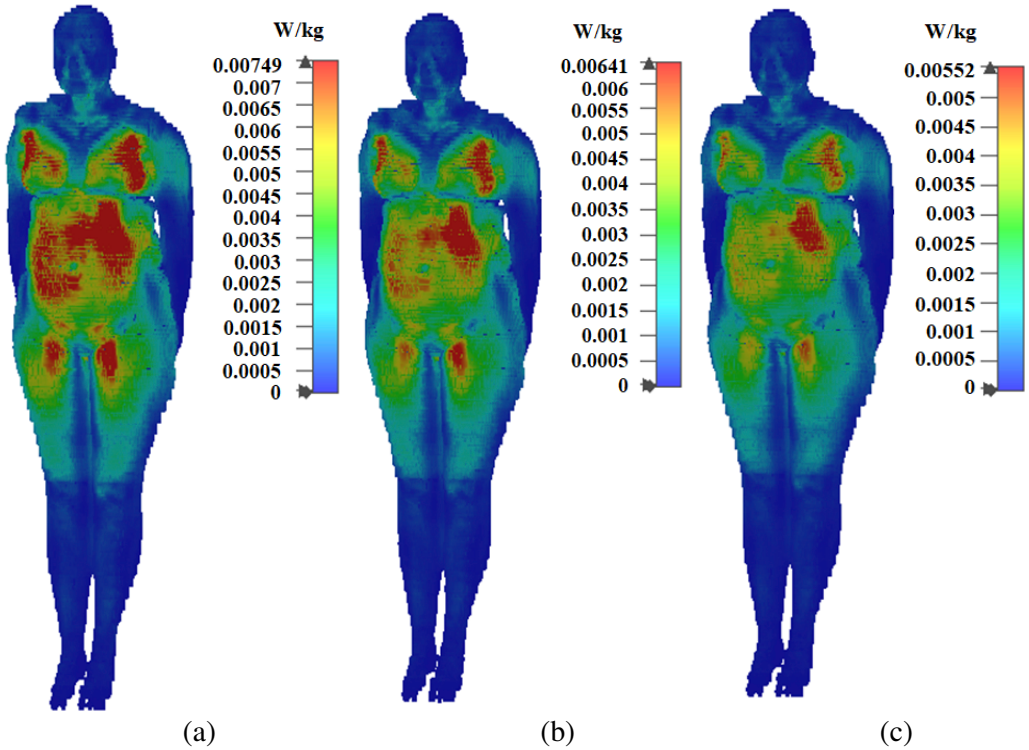

Figure 7. SAR distribution within human at different distance between human body and Wi-Fi device. (a) 10 cm, (b) 30 cm, (c) 50 cm.

wireless accessing internet. Generally, SAR value depends on different parameters, such as the distance between equipment and human body and the radiation intensity. The maximum SAR value described in the IEEE guidelines is 1.6 W/kg for an average mass of 1 g. In the standard ICNIRP, the maximum SAR value is specified as 2 W/kg for an average mass of 10 g. Figure 7 shows the distribution of SAR values when the distances between the human body and Wi-Fi device are 10 cm, 30 cm, and 50 cm in the aluminum alloy carriage.

The relationship between the inducted electric field and the Specific Absorption Ratio (W/kg) is:

$$\mathrm{SAR} = \frac{\sigma |E|^2}{2\rho} \tag{1}$$

where ρ is the mass density of human body tissue (kg/m^3), and σ is the conductivity of human body tissue (S/m).

Electric field strength is the property of electric field in itself. It depends on the input power of the wave source and the distance between wave source and measured point. As can be seen from Figure 7, when the distance is 10 cm, the SAR value within human is higher. Based on Eq. (1), the electric field intensity is proportional to the SAR value. When the human body is very close to the Wi-Fi device, the electric field intensity is strong. It was found that the SAR decreased as the distance increased from the radiating source. The results presented here will assist researchers in examining and simulating the performance of Wi-Fi device in terms of exposure to human tissues. SAR values of main human tissues at 2.4 GHz are shown in Figure 8. Among them, the SAR value of lung is the highest, up to 0.00749 W/kg, far less than the electromagnetic exposure limit of IEEE standard of 1.6 W/kg.

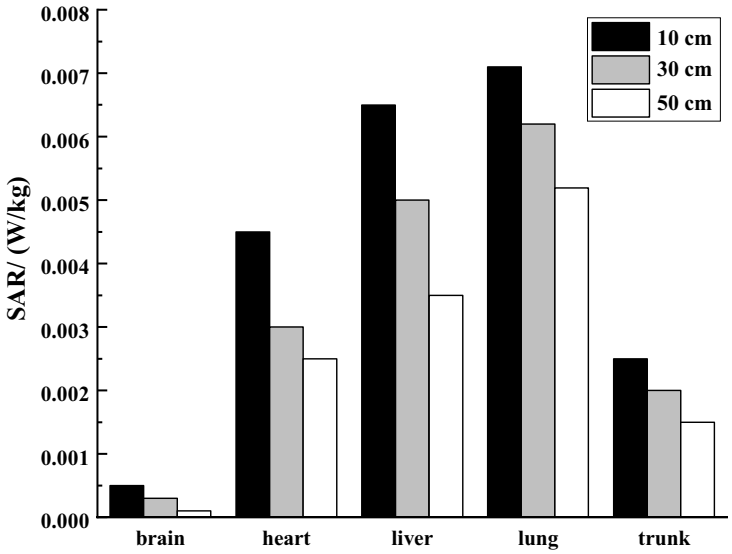

Figure 8. SAR values of main human tissues at 2.4 GHz.

5. CONCLUSION

In order to study the distribution characteristics of low frequency magnetic field of the subway train in complex environment and the electromagnetic exposure of human body, the models of vehicle and human body are established. The nephograms of magnetic flux density in the vehicle with different materials, with or without windows and with the shielding layer are obtained. Then the safety of human electromagnetic exposure in different electromagnetic environments is evaluated. The distribution of SAR within human body in subway train is simulated when the human body and Wi-Fi equipment are at different distances. SAR values of important human tissues are calculated.

The numerical results show that the magnitude and distribution characteristics of the magnetic flux density are related to the vehicle material, windows, and shielding layer. The magnetic flux density

in the region near the interference source is higher than that in other regions. The maximum value of magnetic flux density under different factors is far less than the reference limit of public exposure defined by ICNIRP. The average value of magnetic flux density of the aluminum alloy vehicle reaches 6.3% of ICNIRP limit; that of the CFRP vehicle reaches 5.8% of ICNIRP limit; and that of the stainless steel vehicle reaches 5.4% of ICNIRP limit. The average value of magnetic flux density of the vehicle without windows only reaches 4.9% of ICNIRP limit. The shielding layer can obviously improve the electromagnetic environment, and the average value of magnetic flux density of the vehicle with the shielding layer only reaches 3% of ICNIRP limit. When the Wi-Fi device is closest to the human body, the highest SAR value of human tissue reaches 0.4681% of IEEE limit.

The electromagnetic environment in the subway train will not cause damage to human body in a short time. Therefore, in the early stage of the train design, we should not only ensure that the low-frequency magnetic field is lower than the standard limit, but also consider the mechanical properties of vehicle body materials, the economic benefits of vehicle windows, etc.

REFERENCES

1. "EN 60118-4, Electroacoustics — Hearing aids Part 4: Induction-loop systems for hearing aid purposes — System performance requirements," 2015.
2. "EN 45502-2-1, Active implantable medical devices — Part 2-1: Particular requirements for active implantable medical devices intended to treat bradyarrhythmia (cardiac pacemakers)," 2003.
3. Xu, M., Y. Wang, X. Li, X. Dong, H. Zhang, H. Zhao, and X. Shi, "Analysis of the influence of the structural parameters of aircraft braided-shield cable on shielding effectiveness," *IEEE Trans. Electromagn. Compat.*, Vol. 62, No. 4, 1028–1036, 2020.
4. Liu, G., P. Zhao, Y. Qin, M. Zhao, Z. Yang, and H. Chen, "Electromagnetic immunity performance of intelligent electronic equipment in smart substations electromagnetic environment," *Energies*, Vol. 13, No. 5, 2020.
5. Mo, Y., Y. Wang, F. Song, Z. Xu, Q. Zhang, and Z. Niu, "Investigating the impacts of meteorological parameters on electromagnetic environment of overhead transmission line," *Progress In Electromagnetics Research M*, Vol. 70, 177–185, 2018.
6. Kirsha, A. V. and S. F. Chermoshentsev, "Investigation of the electromagnetic environment in the engine nacelle of an aircraft during the emission of electromagnetic interference from the generator power lines," *Int. Rus. Auto. Conf.*, 1005–1009, 2020.
7. Xie, D., J. Lu, F. Lei, and M. Huang, "Simulation and analysis of radiated electromagnetic environment from cable in cabin," *5th IEEE Int. Symp. MAPE*, 534–537, 2013.
8. Yu, Z., X. Wang, R. Zeng, Y. Fu, L. Liu, and M. Li, "Analysis of factors influencing the parameters of electromagnetic environment," *Institution of Engineering and Technology*, Vol. 2019, No. 16, 2787–2789, 2019.
9. Fady, B., J. Terhzaz, A. Tribak, and F. Riouch, "Integrated miniature multiband antenna designed for WWD and SAR assessment for human exposure," *Int. J. Antennas Propag.*, Vol. 2021, 2021.
10. "ICNIRP statement on the "Guidelines for limiting exposure to time-varying electric, magnetic, and electromagnetic fields (up to 300 GHz)"," *Health Phys.*, 2009.
11. "IEEE standard for safety levels with respect to human exposure to radio frequency electromagnetic fields, 3 kHz to 300 GHz," *IEEE Std C95.1*, 1999.
12. Arduino, A., O. Bottauscio, M. Chiampi, L. Giaccone, I. Liorni, N. Kuster, L. Zilberti, and M. Zucca, "Accuracy assessment of numerical dosimetry for the evaluation of human exposure to electric vehicle inductive charging systems," *IEEE Trans. Electromagn. Compat.*, Vol. 62, No. 5, 1939–1950, 2020.
13. Migliore, M. D. and F. Schettino, "Power reduction estimation of 5G active antenna systems for human exposure assessment in realistic scenarios," *IEEE Access*, Vol. 8, 220095–220107, 2020.
14. Senic, D., A. Sarolic, C. L. Holloway, and J. M. Ladbury, "Whole-body specific absorption rate assessment of lossy objects exposed to a diffuse field inside a reverberant environment," *IEEE Trans. Electromagn. Compat.*, Vol. 59, No. 3, 813–822, 2017.

15. Sadamitsu, S., S. W. Leung, W. K. Lo, and W. N. Sun, "Practical considerations of human exposure in railway systems," *2018 IEEE International Symposium on Electromagnetic Compatibility and 2018 IEEE Asia-Pacific Symposium on Electromagnetic Compatibility (EMC/APEMC)*, 28–31, 2018.
16. "IEEE guide for the measurement of quasi-static magnetic and electric fields," *IEEE Std 1460-1996*, 1997.
17. Gong, M., "Design, simulation and experimental study on electromagnetic shielding structure of carbon fiber reinforced composites for railway vehicles," Beijing Jiaotong University, 2019.